TECHNICAL ARTICLE

Design of a Functional Active Epoxy Coating for Anticorrosion Performance Using SiO$_2$ Nano-Conductive Polyaniline Nanoparticles in Aluminum Blends of Helicopters

S. ABOLFAZL MOKHTARI [ORCID],[1,3] MEHDI SIMIARI,[2] and KAZEM IMANI[1]

1.—Flight and Engineering Department, Imam Ali University, Tehran, Iran. 2.—Faculty of Basic Sciences, Imam Ali University, Tehran, Iran. 3.—e-mail: s.abolfazl.mokhtari@aut.ac.ir

In this study, polyaniline (PANI) nanocomposites/silica (SiO$_2$) nanoparticles are used in epoxy to create smart anticorrosive coatings for the alloy used in helicopters. SiO$_2$ was synthesized by a sol–gel method with tetraethyl orthosilicate. Then, PANI/SiO$_2$ nanocomposites were formed by the electrostatic method. Various tests, including Fourier-transform infrared, ultraviolet–visible spectroscopy, x-ray diffraction, thermo-gravimetric analysis and field-emission scanning electron microscopy, have been performed for characterization of the nanocomposites, and the results indicate that the synthesis of these nanocomposites has been completed. Then, 1 wt.% of PANI/SiO$_2$ nanocomposite was added into epoxy resin and cured by polyamine hardener. Epoxy/PANI/SiO$_2$ coatings with 30-μm thickness were tested on the alloy of the helicopter body. The atomic weight fraction of the helicopter alloy was determined by the inductively-coupled plasma emission test. The results indicate that aluminum constitutes 98% of the alloy. Finally, the analysis of the sealed coatings by electrochemical impedance spectroscopy and salt spray tests have demonstrated that epoxy/polyaniline/silica nanocomposites significantly increase the anticorrosive properties of the epoxy.

Abbreviations

FTIR	Fourier-transform infrared
UV	Ultraviolet–visible spectroscopy
XRD	X-ray diffraction
TGA	Thermo gravimetric analysis
FESEM	Field-emission scanning electron microscopy
EIS	Electrochemical impedance spectroscopy
ICP	Inductively-coupled plasma emission test
PANI	Polyaniline
APS	Ammonium persulfate
TEOS	Tetraethyl orthosilicate

INTRODUCTION

Currently, significant amounts of metals and alloys are used in various industries, and their protection against scratches and corrosion is

considered extremely important.[1–5] There are different ways to inhibit or diminish the generation rate of corrosive components. One of the most efficient methods to prevent metal corrosion is to use organic coatings on the metal surface. The science of coating with many paints and resins is now utilized to protect metals and prevent body corrosion of industrial devices. In order to increase the corrosion resistance of the surface, there are numerous corrosion inhibitors and nanofillers which enhance their long-term weathering performance.[6–10] Preventing corrosion of alloys used in helicopter structures and the process of self-healing and automatic fixation of minor damage, without having to apply traces on alloy structures or any other physical interventions, have become topics of interest for researchers.[11–17]

Aluminum accounts for a significant weight fraction of the exterior helicopter body. This element is frequently used in many industries, devices, vehicles, and helicopters thanks to its low weight and cost. However, its corrosion resistance needs to be enhanced in corrosive environments.[1] Corrosion poses a serious threat to the economy and industry,

Design of a Functional Active Epoxy Coating for Anticorrosion Performance Using SiO$_2$ Nano-Conductive Polyaniline Nanoparticles in Aluminum Blends of Helicopters

1119

and results in potential danger to the environment. Therefore, corrosion protection has become a critically important issue.[18–25] Protection of substrates over surfaces has been achieved by utilizing organic coatings to increase their performance and appearance. In order to reduce the harsh impacts of outdoor exposure, exterior coatings are usually applied. The main destructive factors that damage coatings are corrosion and weathering factors (i.e., temperature, sunlight, water, etc.). These factors not only destroy the coating itself but also cause coating malfunction during service life. As a solution to improve the corrosion resistance of metals, epoxy coatings are among the main useful corrosion protective elements in the industry, with enhanced properties of adhesion, mechanical and tribological strength, and chemical resistance. Polyaniline is a famous conductive polymer that has a simple synthesis, with high stability and low cost. Also, PANI (polyaniline) has several characteristics that can be used for enhanced resistance to corrosive agents.[26–34] Moreover, studies have indicated that utilization of conductive polymers such as polyaniline increases self-healing properties of epoxy coatings. SiO$_2$ nanoparticles have been used in many applications, like organic epoxy coatings, and have gained high attention thanks to their strong scratch resistance, high transparency, and low refraction.[35–49]

Evaluating elements existing in alloys used in helicopter structures via inductively-coupled plasma spectroscopy analysis (ICP), in this study we examine the effects of adding polyaniline nanocomposites and silica nanoparticles to components of epoxy and polyamine film on the self-healing properties of epoxy resin. Polyaniline nanocomposites are synthesized through a solution method using silica nanoparticles. The synthesized nanocomposite structure is then identified via tests including field-emission scanning electron microscopy (FE-SEM), Fourier transform infrared spectroscopy (FT-IR), x-ray diffraction (XRD), UV–visible spectroscopy (UV–Vis), and thermogravimetric analysis (TGA). Self-healing and protective properties of epoxy coatings containing the mentioned nanocomposites are examined via electrochemical impedance spectroscopy (EIS) and salt spray analysis. The results demonstrate that, by applying scratches and rupture of silica nanoparticles, film components are released and curing reactions occur in the scratches, which are finally healed on the coating.[5–7]

MATERIALS AND METHODS

Raw Materials

The alloy used in helicopter structures was supplied by Army Aviation. A 20,000 thinner produced by Iran Pars Kimia was used to decolorize the structure alloy. To this end, 200-, 400-, and 800-grit sandpapers were used. Aniline, ammonium persulfate, and HCL 35% were supplied by the Merck, Germany. Silica nanoparticles were synthesized through a sol–gel method using triethyl orthosilicate supplied by Sigma Aldrich, and ethanol, acetic acid, and ammonium 25% solution were supplied by Merck. Epoxy resin of 828 type supplied by Epicoatand Epicure's E-205 polyamine were used as polymer matrices. For this purpose, epoxy was constantly mixed with polyamine with a 2 to 1 stoichiometry weight/weight percentage.

Synthesis Method of Silica Nanoparticle

An amount of 0.5 mL of acetic acid was added to a flask containing 50 mL of ethanol. The pH was adjusted to 4–4.5 after 1 min. Then, 1 mL of tetraethyl orthosilicate was added to the solution and stirred for 3 h by a magnetic mixer at 30°C. Next, 5 mL of distilled water was added to the solution, and 5 mL of ammonia was instilled after half an hour. An opal solution was formed after 6 h. Sediments were oven-dried at 70°C, after being centrifuge-rinsed with a water:ethanol mixture of 1:4 volume proportions at 3000 rpm for half an hour, and for five consecutive times.[1–4]

Synthesis Method of Polyaniline Nanocomposite and Silica Nanoparticles

Polymerization was performed via an electrostatic method using a 1 M solution of hydrochloric acid. The amount of 10 m^3 of hydrochloric acid was increased to 120 m^3 by adding distilled water. Then, 110 m^3 of the solution was mixed with 0.1 g of silica nanoparticles and ultrasonicated by a homogenizer at 200 W for 60 s. The mixture was then stirred for 30 min. An ice-water bath was prepared, and the system was sealed in the presence of totally oxygen-free nitrogen gas. Aniline was injected into the system with a syringe through a thread-sealing tape so as to avoid nitrogen depletion from the system, and then stirred for 30 min. Next, 10 m^3 of the remaining hydrochloric acid solution from the previous stage was stirred for 10 min with 1.24 g of ammonium persulfate until it was thoroughly dissolved.[1–8]

The resulting solution was then injected into the mixture through a syringe pump, dripping with an approximate rate of one drop per 5 s. It was observed during the injection that the solution color turned from light yellow to brown, then blue, and finally green. The solution was next stirred for 6 h at 0–4°C. Finally, the resulting solution was transferred to a beaker, stored in a refrigerator for polymerization to continue for another 24 h, and for the remaining oligomers to turn into polymer, and for the reaction to end. The nanocomposite from the previous step was centrifuged three times at 3000 rpm for 30 min with a 3:1 mixture of deionized methanol:water. The rinsed nanocomposites were dried for 24 h at 45°C.[39,41,50–52]

Preparation Method of Nanocomposite Coating Using Epoxy Resin

In order to prepare a polymeric nanocomposite as the coating complying with the research, metallic surfaces of the alloy to be coated were prepared. To do this, the metallic surface was polished using 400-, 800-, and 1200-grit sandpapers. The plates were subsequently exposed to ultrasonic waves in acetone and methanol to ensure that the metal surface was entirely degreased and cleaned. Three types of coating were processed during this study, namely fine epoxy, epoxy–nanosilica composite, and epoxy–polyaniline nanocomposite/silica composite with 1 wt.% of nanoparticles. To obtain a pure epoxy coating, epoxy resin and amine hardener with 2:1 weight proportion were mixed for 10 min. The work process in preparation of the epoxy–nanosilica composite was as follows: 3 g of resin was mixed with 45 mg of oxidized diamond nanoparticles, and the resulting mixture was stirred under amalgamation in a mixer at 1000 rpm for 30 min to obtain an even distribution of nanoparticles in the epoxy resin. Sonication was thereafter performed on the mixture for 7 min (2 min pulse-on and 5 min pulse-off) to disperse the nanoparticles and to eliminate bubbles. At the next stage, 1.5 g of amine hardener was added to the mixture followed by amalgamation for 10 min, so that the nanocomposite with 1 wt.% nanoparticles would come out.[12–15]

The epoxy–polyaniline composite/silica composite formation sequences are exactly the same. The only difference is that the polyaniline-containing nanocomposite was used instead of nanosilica. Subsequently, the mixture was exposed to air for trapped bubbles to completely escape, and also for its viscosity to be slightly enhanced. Ultimately, a 30-μm layer was applied to the finished metal surface using a film applicator. The obtained coating was initially heated in an oven at 55°C for 2 h to reach the gelling point, followed by heating at 100°C for 1 h to accomplish additional curing. Finally, the coating was stored in ambient temperature for 1 week to ensure the completion of the curing procedure. To perform electrochemical impedance tests, a 1×1 cm^2 profile of the coating was selected and the rest of the metallic plate was caulked by a scalded mixture of beeswax and colophony. However, an uncoated corner of the metal was left bare to serve as an electrode connector. A 3.5 wt.% water and salt solution was prepared in which the coatings were immersed, and impedance test was performed on the coating at regular intervals.[4,6,9,18,44,53–55]

RESULTS AND DISCUSSION

The Field-Emission Scanning Electron Microscopy Test (FESEM)

The scanning electron microscope functioning mechanism scans the sample surface with a set of high-energy electron beams to generate images. Based on these images, information concerning surface morphology, crystal structure of the particles, and the particle and crystal expansion and growth direction can be extracted. Non-conductive materials are usually covered with a layer of gold or a gold alloy. In this way, the quality of the images will be enhanced. For FE-SEM imaging, the samples should be free of moisture, organic solvents, and grease layers. The test was performed using a TESCAN-MIRA III FE-SEM (Czech Republic). Since the samples were non-conductive, a gold coating was applied. The results in scales of 2 μm, 1 μm, and 500 nm indicated that polyaniline is formed along with the silica nanoparticles in a diameter of approximately 150–200 nm. The results obtained from the microscopic imaging indicated the formation of polyaniline among silica nanoparticles. The images in Fig. 1 demonstrate the morphology and positioning of polyaniline around silica nanoparticles.[7,56–59]

The Fourier-Transform Infrared Spectroscopy Test (FT-IR)

In this study, this test was performed for each sample using an ABB-Bomem MB-100 spectrometer. FT-IR analysis was applied to characterize the chemistry of the silica and PANI/silica. FT-IR spectra were obtained in the range of 4000–400 cm wavenumber via a KBr pellet method. Further, the depicted absorbance bonds including the bending vibration of NH_2 (3173 cm^{-1}), asymmetric vibration, and bending vibration of the Si-O-Si and Si-OH network (1120 cm^{-1} and 614 cm^{-1}) and Si-OH (1073 cm^{-1}) are shown in Fig. 2[5,23–25].

In addition, the appearance of a carbon–nitrogen bond stretching at 1304 cm^{-1} can verify the covalent bonding of polyaniline on the silica nanoparticles through reaction with an epoxide ring existing on the basal plane of SiO_2. For salty-state polyaniline, the peak witnessed in the range of 3350–3288 is related to asymmetric tensile bonding of nitrogen–hydrogen. The absorption peak at 1680 is a vibrational tensile peak of carbon–carbon bond, and the peak at 1557 is a tensile carbon–carbon bond of aromatic ring. The peak present at 1460 is related to a dual tensile bond of aromatic compound carbons. The peak at 1282 is a secondary tensile carbon–nitrogen bond of aromatic amines. Therefore, it can be generally said that the infrared spectrum and presence of peaks in range of 3100–3400 are indicative of the presence of hydroxyl bonds, and the presence of silica–oxygen bonds and nitrogen–hydrogen bonds imply the formation of polyaniline. Also, the peaks present in range of 900–1300 demonstrate the presence of bonds in the silica nanoparticles, which in turn indicate the formation of the silica/polyaniline nanocomposite. The results obtained from the
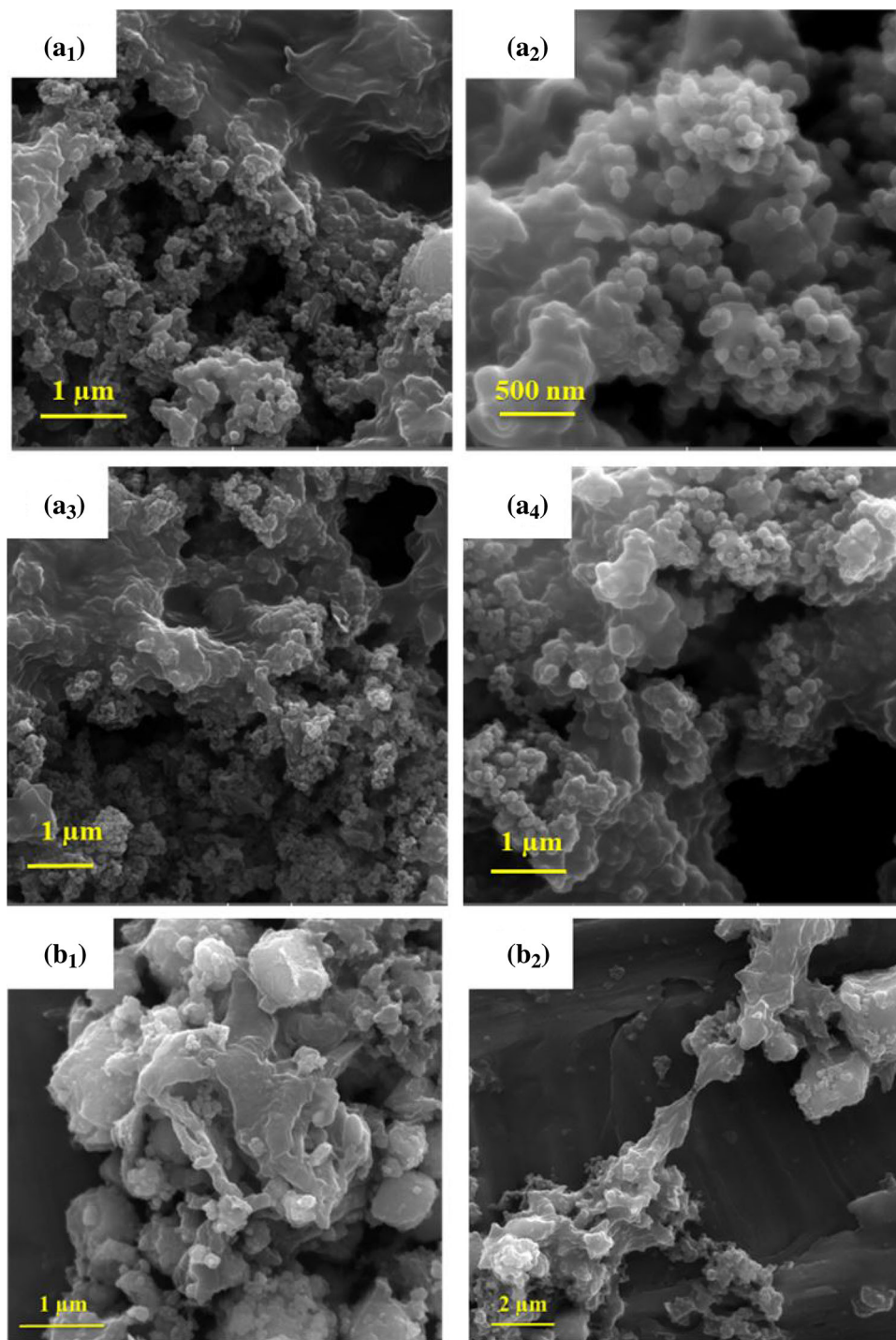
Fig. 1. Images of the field emission scanning electron microscope: (a_1), (a_3), and (a_4) display the polyaniline/silica nanocomposite at the scale of 1 μm, (a_2) displays the polyaniline/silica nanocomposite at the scale of 500 nm. (b_1) displays the synthesized polyaniline at a scale of 1 μm, and (b_2) the synthesized polyaniline at a scale of 2 μm.

spectrometer show nitrogen–hydrogen, carbon–nitrogen, and silica–hydrogen peaks at 3000 and 1300–1100, respectively. This proves that polyaniline has formed a nanocomposite with silica nanoparticles as an in situ polymerization.

X-ray Diffraction Spectroscopy Test (XRD)

In this study, the samples were characterized by an XRD device, Mira 3—XML, TESCANCzech Republic). The presence of a sharp peak at the double of the theta angle around 20–25 indicates the
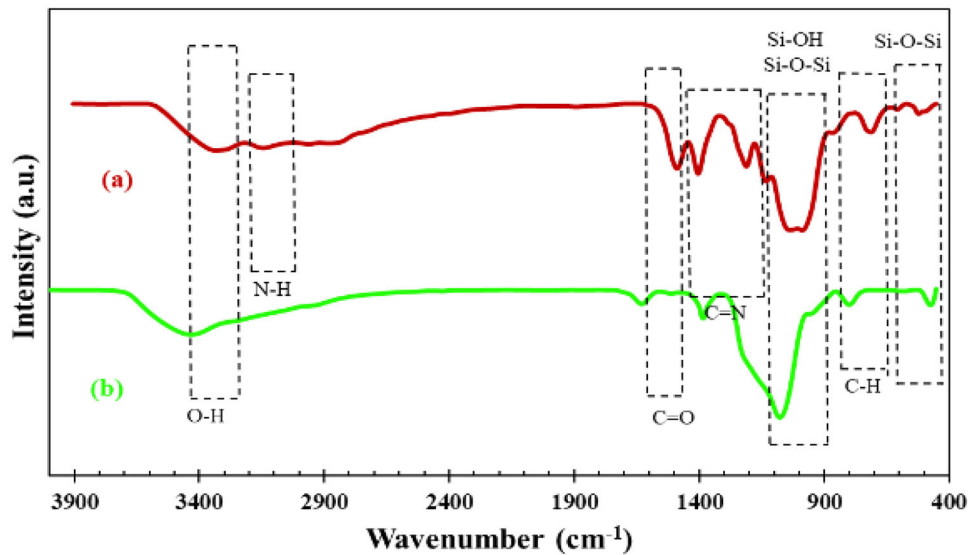
Fig. 2. Infrared test spectrum: (a) the red peak indicates polyaniline/silica nanocomposite, and (b) the green peak is for silica nanoparticles (Color figure online).
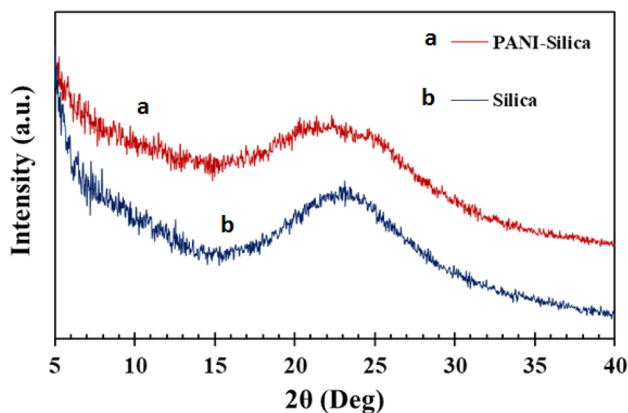

Fig. 3. X-ray diffraction test: (a) the red peak indicates the polyaniline/silica nanocomposite, and (b) the blue peak is related to the silica nanoparticles (Color figure online).

Fig. 4. UV spectrum of polyaniline and polyaniline/silica nanocomposite.

formation of polyaniline, and the shift of the diagram of the polyaniline–silica nanocomposite is indicative of the presence of these nanoparticles (Fig. 3). In order to analyze the crystalline structures, SiO_2 and polyaniline/silica XRD analyses were carried out. The identified SiO_2 nanoparticles and $PANI/SiO_2$ nanocomposites are shown in Fig. 3 where the peak at $2\theta = 22.5$ indicates that the PANI has caused a shift in peak to $2\theta = 21.5$, and created a sharper peak than that from silica.[6,26,27]

UV–Vis Spectroscopy (UV–Vis)

A UV–Vis Spectrometer (T90+: PG Instruments) was used to conduct this test. The electronic structure of polyaniline and polyaniline/silica nanocomposites can be studied through UV–vis analysis, as shown in Fig. 4. According to the figure, it can be seen that polyaniline and its composites have two
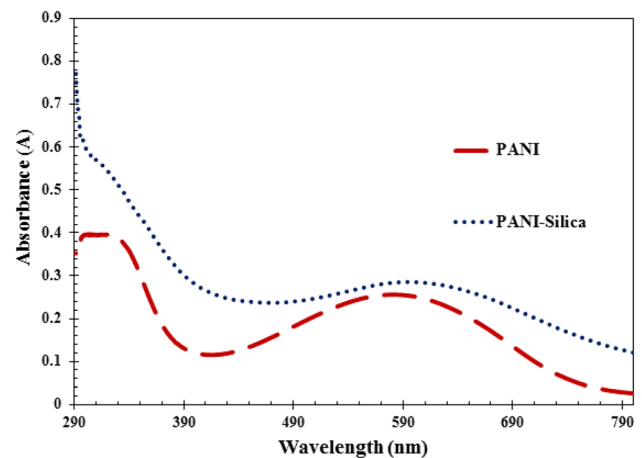
major peaks: one at 350 nm and the other at 640 nm. The former is related to a transition zone within the benzenoid ring, and the latter is associated with a polaron transition bond within the quinoid ring. The polaron transition zone comes into sight when a conducting form of polyaniline, like its salty state, is present in a compound. The presence of two $\pi-\pi$ bond peaks around 350 and others around 400 and 600 imply the formation of polyaniline and its nanocomposite with silica nanoparticles.

Thermogravimetric Analysis (TGA)

In order to evaluate the presence of functional groups on the surface of PANI and $PANI/SiO_2$, TGA tests were performed using a Mettler Toledo TGA/DSC device in a nitrogen-dominant atmosphere with a heating rate of 10°C per min, from ambient

Design of a Functional Active Epoxy Coating for Anticorrosion Performance Using SiO₂ Nano-Conductive Polyaniline Nanoparticles in Aluminum Blends of Helicopters
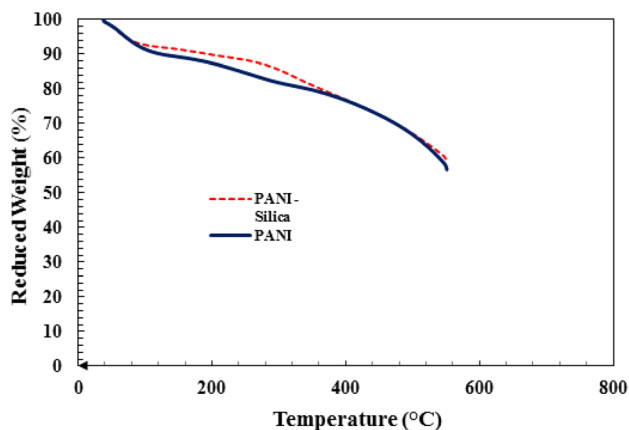
1123

Fig. 5. Thermogravimetric analysis and weight loss of polyaniline/silica nanocomposite by increasing the temperature.
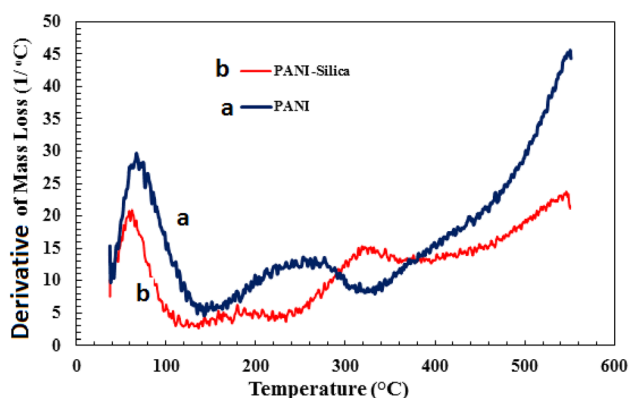

Fig. 6. Thermogravimetric analysis and weight loss rate for (a) polyaniline and (b) silica nanocomposite in terms of 1/°C.

temperature up to 600°C. TGA/DTG was employed for this purpose. Figure 5 presents the TGA and derivative TG (DTG) curves of PANI and PANI/SiO_2. As shown in Figs. 5 and 6, for PANI and PANI/SiO_2 samples at 100°C, the water in the samples has been evaporated and about 8% weight of the samples is lost. By increasing the temperature of PANI/SiO_2, the existence of silica nanoparticles leads to a lower percentage weight reduction than when only PANI is used. Beyond 380°C, some SiO_2 chemical bonds were destroyed and the two samples became similar (Fig. 5).[22,25–27]

The first degradation is probably due to moisture, aniline monomer, or phosphoric acid dopants. The second weight loss is related to degradation of the polymer chains. Regarding DTG analysis and studies in this field, it may be perceived that the peak present in the temperature range of 100–300°C is related to heat degradation of the amine groups. Additionally, the peak present at 327°C is related to the amide groups.[19,21,25]

Inductively Coupled Plasma Emission Test (ICP)

Conducting polymers like PANI are used on metals such as aluminum alloys and mild steel. In order to determine the weight fraction of elements in the alloy of the helicopter exterior body, and to determine its appropriate coating, ICP analysis was carried out by 70 elements using an ICP-OES 730-ES, Varian device. The results indicate that the helicopter body consists of 98% aluminum, 0.66% magnesium, 0.46% iron, 0.31% chromium, etc. The results are presented in Table I.[3,28,29]

Electrochemical Impedance Spectroscopy (EIS)

The Corr Test CS350 was used to perform the EIS test. A frequency range of 0.1–10,000 Hz was selected to measure the electrochemical impedance, and a Bode diagram was used to inspect corrosion resistance. In the Bode diagram, the absolute values of the impedance and the phase angle of the system are drawn in a logarithmic scale in terms of the frequency. Three working, reference, and auxiliary electrodes were used in the electrochemical cell, and Zview software was used to compare equivalent diagrams. Using the Bode diagram, three coatings were derived including pure epoxy, epoxy–nanosilica, and epoxy–polyaniline/silica nanocomposite, shown, respectively, in Supplementary Figs. S.1, 2, 3. As pointed out earlier, the impedance rate is our measurement criteria in frequencies as low as 0.1 Hz. According to Supplementary Fig. S.1, the impedance rate of the coating at 0.1 Hz frequency is observed as being in a higher to lower rate sequence for pure epoxy. However, for the nano-silica epoxy sample, the impedance rate drops with time. The decline of the constant impedance rate with time, as seen for this sample, indicates that the corrosion inhibitor has failed to sufficiently become released out of the nanoparticles, or its concentration in the electrolyte solution has not been high enough to form a protective film on the metallic surface and subsequently increase the impedance rate. However, after the inhibitor is released in self-healing systems, the electrochemical resistance increases with time.

The capabilities of SiO_2 and PANI/SiO_2 nanoparticles, which are added into epoxy resin, were manifested by EIS measurements on non-defected samples. For this purpose, three samples were prepared, and the results of these samples are compared for various immersion times (5 days, 18 days, 43 days, 57 days, 71 days, and 85 days). Impedance in the lowest frequency ($|Z|$ 10 m Hz), is attributed to the aluminum samples exposed to 3.5% NaCl solutions, neat epoxy, epoxy/SiO_2, and epoxy/PANI/SiO_2. Overall, the nanocomposite coatings containing SiO_2 and SiO_2/ PANI nanoparticles showed the highest resistance against corrosive

Table I. Weight percentage combination of the elements of the exterior helicopter body alloy, according to the inductively-coupled plasma spectroscopy

Element	Weight fraction %	Element	Weight fraction %
Al	98	Ti	0.02
Mg	0.66	K	0.02
Fe	0.46	S	0.0095
Cr	0.31	Ga	0.007
Cu	0.22	Ni	0.0054
Sr	0.11	B	0.0038
Zn	0.1	Zr	0.0036
Mn	0.073	Ba	0.0026
Si	0.044	Cd	0.00047
Ca	0.043		

agents with respect to neat epoxy (see supplementary Figs. S.1, 2, 3).

Salt Spray Test

To examine the electrochemical application of the samples, the coated plates were exposed to a saline fog chamber and, subsequently, a salt spray test was conducted on the nanocomposite coating with the results reported up to 10 days (Supplementary Fig. S.4). With increasing exposure time, a higher portion of corrosion products was generated around the scribed region, exhibiting the corrosive species diffusion into the interface of the aluminum coating and the electrochemical reactions occurring beneath the epoxy coating. The salt spray test results prove that the coating reinforced by SiO_2/PANI nanoparticles exhibited a better corrosion protection performance against the salt spray test conditions with less coating delamination, rust, and blistering.[14,15,32,36]

In order to evaluate the functionality of the coatings, samples with an area of 8×10 were exposed to spraying a 5 wt.% salt solution. The images taken from samples indicate that the scratch created in the sample with the epoxy and SiO_2/PANI nanocomposite was far less than that in samples with epoxy and epoxy/SiO_2. After performing the salt spray analysis, the results were matched with the electrochemical impedance test (see supplementary Fig. S.4).

CONCLUSION

The characterization of SiO_2 and SiO_2/PANI nanoparticles was carried out by FT-IR, UV–vis, XRD, TGA, and finally FE-SEM analysis. The results clearly showed that the polymerization was significantly carried out around SiO_2 nanoparticles. The synthesized nanoparticles were incorporated into the epoxy coating, and then common electrochemical analyses, such as EIS and a salt spray test, were conducted to uncover the effect of the SiO_2 nanoparticles on the capacity of the sample of the anticorrosive agent. The outcome has exactly shown that the addition of the SiO_2 and SiO_2/PANI

nanoparticles to the epoxy coating directly affected the anticorrosion properties of the coating in the intact samples. Overall, the results of this research demonstrated that synthesis of polyaniline nanocomposites and silica nanoparticles has been performed perfectly. Moreover, the ICP test indicates the precise weight percentage of elements contained in the alloy used for helicopter structures. Using this information and other existing sources, and according to the EIS test and salt spray test results, it is concluded that incorporating polyaniline/silica nanocomposites into the samples improves the self-healing properties of epoxy resin, which in turn reduces corrosion in alloys used in helicopter structures.

FUNDING

DATA AVAILABILITY

All data reported in this research are available upon request to the corresponding author.

CONFLICT OF INTEREST

On behalf of all the authors, the corresponding author states that there is no conflict of interest.

SUPPLEMENTARY INFORMATION

The online version contains supplementary material available at https://doi.org/10.1007/s11837-021-04565-6.

REFERENCES

1. C.M. Correa, R. Faez, M.A. Bizeto, and F.F. Camilo, *RSC Adv.* 2, 3088 (2012).
2. M. Izadi, T. Shahrabi, I. Mohammadi, B. Ramezanzadeh, and A. Fateh, *Compos. Part B Eng.* 171, 96 (2019).
3. S. de Souza, S. de Souza, *Surf. Coat. Technol.* 201, 7574 (2007).

Design of a Functional Active Epoxy Coating for Anticorrosion Performance Using SiO₂ Nano-
Conductive Polyaniline Nanoparticles in Aluminum Blends of Helicopters
1125

4. S.A. Haddadi, M. Mahdavian, and E. Karimi, *RSC Adv.* 5, 28769 (2015).
5. T. Rabizadeh, and S.R. Allahkaram, *Mater. Des.* 32, 133 (2011).
6. M.L. Zheludkevich, J. Tedim, and M.G.S. Ferreira, *Electrochim. Acta.* 60, 31 (2012).
7. S.A. Kumar, H. Bhandari, C. Sharma, F. Khatoon, and S.K. Dhawan, *Polym. Int.* 62, 1192 (2013).
8. M.J. Palimi, M. Rostami, M. Mahdavian, and B. Ramezanzadeh, *J. Coat. Technol. Res.* 12, 277 (2015).
9. J.I.I. Laco, F.C. Villota, and F.L. Mestres, *Prog. Org. Coat.* 52, 151 (2005).
10. B. Rossenbeck, P. Ebbinghaus, M. Stratmann, and G. Grundmeier, *Corros. Sci.* 48, 3703 (2006).
11. S. Sadreddini, and A. Afshar, *Appl. Surf. Sci.* 303, 125 (2014).
12. M.A. Ahmed, M.F. Abdel-Messih, and E.H. Ismail, *J. Mater. Sci. Mater. Electron.* 31, 19118 (2019).
13. T. Kosec, A. Legat, J. Kovač, and D. Klobčar, *Coatings* 9, 3390 (2019).
14. A.M. Al-Sabagh, M.I. Abdou, M.A. Migahed, A.M. Fadl, and M.F. El-Shahat, *Adv. Powder Technol.* 29, 367 (2018).
15. N.M. Naim, H. Abdullah, and A.A. Hamid, *Electron. Mater. Lett.* 15, 70 (2019).
16. I. Herrmann-Geppert, J. Radnik, U.I. Kramm, S. Fiechter, and P. Bogdanoff, *ECS Trans.* 136, 978 (2019).
17. S. Ghiyasi, M.G. Sari, M. Shabanian, M. Hajibeygi, P. Zarrintaj, M. Rallini, L. Torre, D. Puglia, H. Vahabi, M. Jouyandeh, F. Laoutid, S.M.R. Paran, and M.R. Saeb, *Prog. Color Colorants Coat.* 11, 199 (2018).
18. F. Dolatzadeh, S. Moradian, and M.M. Jalili, *Color Colorants Coat.* 3, 92 (2011).
19. N. Pirhady Tavandashti, M. Ghorbani, A. Shojaei, J.M.C. Mol, H. Terryn, K. Baert, and Y. Gonzalez-Garcia, *Corros. Sci.* 112, 138 (2016).
20. E. Barna, B. Bommer, J. Kürsteiner, A. Vital, O.V. Trzebiatowski, W. Koch, B. Schmid, and T. Graule, *Compos. Part A Appl. Sci. Manuf.* 30, 899 (2005).
21. S. Sahoo, P.K. Sahoo, A. Sharma, and A.K. Satpati, *Sens. Actuators B Chem.* 309, 127763 (2020).
22. E. Matin, M.M. Attar, and B. Ramezanzadeh, *Color Colorants Coat.* 10, 181 (2015).
23. S. Riaz, M. Ashraf, T. Hussain, and M.T. Hussain, *Cellulose* 26, 5159 (2019).
24. E. Javadi, M. Ghaffari, G. Bahlakeh, and P. Taheri, *Prog. Org. Coat.* 135, 496 (2019).
25. X. Zhang, and S.K. Manohar, *Chem. Commun.* 20, 2360 (2004).
26. H. Yi, C. Chen, F. Zhong, and Z. Xu, *High Perform. Polym.* 15, 893 (2014).
27. H. Zangeneh, A.A. Zinatizadeh, S. Zinadini, M. Feyzi, and D.W. Bahnemann, *Compos. Part B Eng.* 176, 107158 (2019).
28. M. Eid, M.B. El-Arnaouty, M. Salah, E.S. Soliman, and E.S.A. Hegazy, *Inorg. Chem. Commun.* 114, 107844 (2020).
29. A. Habibiyan, B. Ramezanzadeh, M. Mahdavian, G. Bahlakeh, and M. Kasaeian, *Chem. Eng. J.* 391, 123630 (2020).
30. B.W. Walker, R. Portillo Lara, E. Mogadam, C. Hsiang Yu, W. Kimball, and N. Annabi, *Prog. Polym. Sci.* 92, 135 (2019).
31. V.S. Kathavate, and P.P. Deshpande, *Surf. Coat. Technol.* 394, 125902 (2020).
32. Y. González-García, J.M.C. Mol, T. Muselle, I. De Graeve, G. Van Assche, G. Scheltjens, B. Van Mele, and H. Terryn, *Electrochem. Commun.* 5, 2355 (2011).
33. H. Wiggers, Y.H. Sehlleier, F. Kunze, L. Xiao, S.M. Schnurre, and C. Schulz, *Solid State Ionics* 344, 115117 (2020).
34. G. Williams, S. Geary, and H.N. McMurray, *Corros. Sci.* 57, 139 (2012).
35. B.C. Roy, M.D. Gupta, L. Bhoumik, and J.K. Ray, *Synth. Met.* 130, 27 (2002).
36. A.A. Razin, H. Yari, and B. Ramezanzadeh, *J. Ind. Eng. Chem.* 31, 291 (2015).
37. F.L. Jin, X. Li, and S.J. Park, *J. Ind. Eng. Chem.* 29, 1 (2015).
38. O.J. Obies, M.A. Mutar, and R.G. Kadhim, *NeuroQuantology* 18, 96 (2019).
39. M.S. Cho, S.Y. Park, J.Y. Hwang, and H.J. Choi, *Mater. Sci. Eng.* 24, 15 (2004).
40. X. Zhang, W.J. Goux, and S.K. Manohar, *J. Am. Chem. Soc.* 126, 4502 (2004).
41. A. Ghazi, E. Ghasemi, M. Mahdavian, B. Ramezanzadeh, and M. Rostami, *Corros. Sci.* 94, 207 (2015).
42. E. Alibakhshi, E. Ghasemi, M. Mahdavian, B. Ramezanzadeh, and M. Yasaei *J. Clean. Prod.* 251, 119676 (2020).
43. A. Ghazizadeh, S.A. Haddadi, and M. Mahdavian, *RSC Adv.* 6, 18996 (2016).
44. F.F. Wang, Y. Zhang, H. Zhang, L. Xu, P. Wang, and C. Bin Guo, *RSC Adv.* 8, 5268 (2018).
45. A.V.C. de Braga, D.C.B. do Lago, A.R. Pimenta, and L.F. de Senna, *Surf. Coat. Technol.* 372, 190 (2019)..
46. H. Yari, S. Moradian, and N. Tahmasebi, *J. Coat. Technol. Res.* 11, 351 (2014).
47. V. Talwar, O. Singh, and R.C. Singh, *Sens. Actuators B Chem.* 191, 276 (2014).
48. Y. González-García, S.J. García, A.E. Hughes, and J.M.C. Mol, *Electrochem. Commun.* 70, 142 (2011).
49. B. Ramezanzadeh, Z. Haeri, and M. Ramezanzadeh, *Chem. Eng. J.* 303, 511 (2016).
50. L. Huang, P. Zhu, G. Li, D. Lu, R. Sun, and C. Wong, *J. Mater. Chem. A.* 2, 18246 (2014).
51. B. Sixou, J. Travers, C. Barthet, and M. Guglielmi, *Phys. Rev. B Condens. Matter Mater. Phys.* 56, 4722 (1997).
52. Y.J. Wan, L.C. Tang, L.X. Gong, D. Yan, Y.B. Li, L. Bin Wu, J.X. Jiang, and G.Q. Lai, *Carbon N. Y.* 69, 467 (2014).
53. A. Alizadeh Razin, B. Ramezanzadeh, and H. Yari, *Prog. Org. Coat.* 92, 95 (2016).
54. Y.Y. Horbenko, B.R. Tsizh, O.I. Aksimentyeva, I.B. Olenych, V.M. Bogatyrev, and M.R. Dzeryn, *Sci. Messenger LNU Vet. Med. Biotechnol.* 21, 96 (2019).
55. L. Al-Mashat, K. Shin, K. Kalantar-Zadeh, J.D. Plessis, S.H. Han, R.W. Kojima, R.B. Kaner, D. Li, X. Gou, S.J. Ippolito, and W. Wlodarski, *J. Phys. Chem.* 114, 16168 (2010).
56. I. Fratoddi, I. Venditti, C. Cametti, and M.V. Russo, *Sens. Actuators B Chem.* 220, 534 (2015).
57. R. Ansari, and A.H. Alikhani, *J. Coat. Technol.* 6, 221 (2009).
58. Y. Liao, X.G. Li, E.M.V. Hoek, and R.B. Kaner, *J. Mater. Chem. A.* 1, 11795 (2013).
59. E. Alibakhshi, E. Ghasemi, M. Mahdavian, and B. Ramezanzadeh, *Color Colorants Coat.* 9, 233 (2016).